Cihan University-Erbil Scientific Journal (CUESJ)

REVIEW ARTICLE

The Comparative Study of Biaxial Bending Analysis of Steel Sections Using AISC and Eurocode Approaches

Mohammed M. Saleh[1]*, Dlshad K. Ahmed[2], Ali R. Yousef [3]

[1]*Department of Civil Engineering, Engineering Collage, Universita della Calabria, Cosenza, Italy,* [2]*Department of Civil Engineering, Cihan University-Erbil, Kurdistan Region, Iraq,* [3]*Department of Civil Engineering, Engineering Collage, Salahaddin University, Erbil, Iraq*

ABSTRACT

This study investigates the capacity of the steel section using both AISC and Eurocode approaches. Three types of steel sections were subjected to biaxial bending by applying loads to both main axes and examined by both approaches. The concept of Fisher was also adopted as an approach. This concept proposed that only the compression flange could withstand lateral loading and the torsional influence could be ignored. The findings suggested that the Eurocode approach is more conservative in the design of steel sections subject to biaxial bending as it takes into account the level at which the load is applied, the type of the section whether rolled or welded and its height-to-width ratio (lateral buckling effect). The AISC approach considers the shear center of the section as the level at which the loads are applied. The conservatism of the results was more pronounced when the section is close to H-section. Fisher`s concept of structural design of biaxial bending of structural steel is more conservative than both AISC and Eurocode approaches of analysis.

Keywords: AISC specification, biaxial bending analysis, eurocode, fisher`s concept, steel sections

INTRODUCTION

Due to many factors, such as good mechanical properties, quick and easy construction and economy, steel structures are commonly used for construction. Overhead crane runway girders are examples of biaxial bending in which bending moments applied to both major and minor axis. When the loads applied through the shear center, twisting would not develop[2] as shown in Figure 1. For this case, AISC 360 Commentary,[1] biaxial bending equation given by the AISC 360 Eq. (H1-1b) by supposing of axial load that equal to one. The interaction equation then reduces to

$$\frac{M_{ry}}{M_{cy}} + \frac{M_{rz}}{M_{cz}} \leq 1 \qquad (1)$$

where

M_{ry} = applied bending moment (y-axis), M_{cy} = nominal moment capacity (y-axis), M_{rz} = applied bending moment (z-axis), M_{cz} = nominal moment capacity (z-axis). For the LRFD method, $Mc = \Phi_b M_n$, while for ASD method, $Mc = M_n/\Omega_b$, $\Phi_b = 0.9$ = factor for resistance in flexure, $\Omega_b = 1.67$ = safety factor for flexure.

Regarding to the bending about the strong axis, the Eurocode method focused on several factors that could affect the flexure strength of the beams. The Elastic Critical Moment is valuable for the study of lateral-torsional beam buckles. The maximum bending moment value provided by the beam

is described as this quantity, far from imperfections of some kind.

$$M_{cr}^E = \frac{\pi}{L}\sqrt{G I_T E I_z \left(1 + \frac{\pi^2 E I_W}{L^2 G I_T}\right)} \qquad (2)$$

where I_T is the torsion constant, Iz is the second moment of area in (weak axis), I_W the warping constant, L is the length between laterally braced cross-sections of the beam, and E and G are the longitudinal modulus and the shear modulus of elasticity, respectively. Because of the different loading types and bending moment diagrams, broad equations can be found in practical implementations and are suitable for a range of conditions, the most widely used in the formulation adopted by the commission,[3] acceptable to members subject to bending moment on a strong axis with a mono-symmetric cross-section

Figure 1: Pure biaxial bending[2]

Figure 2: Lateral load applied on the upper flange
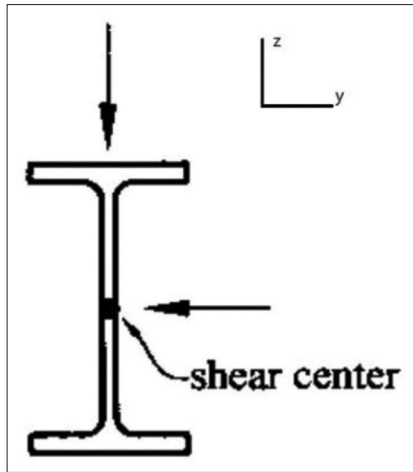
on a weak axis. For the calculation of the elastic critical moment under criteria not covered by Boissonnade *et al.*[3]

$$M_{cr} = C_1 \frac{\pi^2 E I_z}{(K_z L)^2} \left\{ \left[\left(\frac{k_z}{k_w} \right)^2 \frac{I_w}{I_z} + \frac{G I_T}{\pi^2 E I_z} + \frac{(k_z L)^2 \left(C_2 z_g - \right)^2}{\left(C_3 z_j \right)} \right]^{0.5} - \left(\frac{C_2 z_g -}{C_3 z_j} \right) \right\}$$

(3)

The shape of the bending moment diagram gives the coefficient of C_1, C_2, and C_3, support conditions give the coefficients k_z and k_w which are called the effective length factor, $z_g = (z_a - z_s)$, Where z_a and z_s, comparable to the centroid of the cross-section, are the locations of the point of applied load and the shear center; these amounts are positive if the compressed portion is placed and negative if the tension portion is placed. While AISC requirements lead us to calculate the capacity of the bending moment without taking into account the level of load application,[1] even the steel section is rolled or welded.[4] The lateral load is also added to the compression flange of the member, as shown in Figure 2. In this case, the conceptual solution proposed by Fisher should be used,[5] this concept assumed that only the compression flange can survive lateral loading and the torsional impact can be ignored. In the case of I-shapes, the plastic section modulus of a Z-axis flange is provided by

$$Z_t = \frac{Z_z}{2}$$

(4)

Where Z_z is plastic section modulus about the Z-axis. The moment capacity of one flange about the Y-axis is

$$M_{nt} = F_y \times Z_t$$

(5)

Linear additions of the moment terms in[1] as shown in Figure 3 typically lead to results which are too conservative.[6] Based on the definition on biaxial bending, we will extend this to one case of study using both AISC and Eurocodes to investigate and demonstrate the deference between them regarding the level at which the load is applied, the type of the section whether rolled or welded and its height-to-width ratio by evaluating the results using Robot Structural Analysis software.
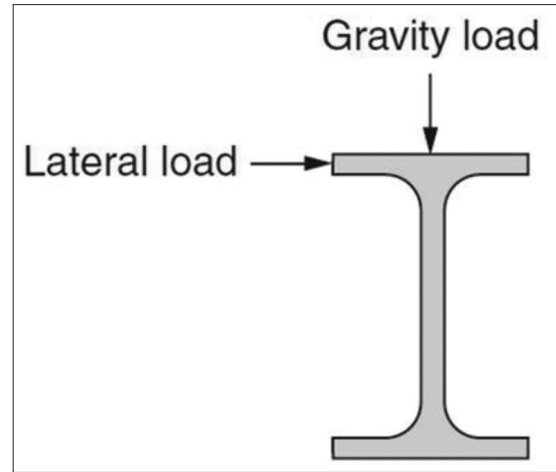
METHODOLOGY

To demonstrate the exact difference between AISC and Eurocode analysis methods regarding biaxial bending, the case of study struggles with the loads added to the upper flange as shown in Figure 1, and Fisher's concept[5] will be regarded. The case study includes a simply supported beam with a span of 10.0 m, measured center-to-center of support, with the load being applied at midspan, as shown in Figure 4, the beam under consideration is subjected to vertical load and the lateral load with the value 25 kN and 5 kN, respectively. The beam has yielding strength (f_y = 355 MPa), modulus of elasticity (E = 21×10^3 MPa) and detailed properties are shown in Table 1.

For the common base of comparison, the load factors in both approaches will be based on that of AISC standards.[7]

$$1.2 \, DL + 1.6 \, LL$$

(6)

The applied factored loads (moments) are shown in Table 2. The dead load includes the self-weight of the member as uniformly distributed which is calculated by the software.

AISC Methods of Analysis

For AISC methods of analysis in the Robot structural analysis software, modification factor should be defined for moment gradient C_b in the member definition section which is equal to 1.32 for single point load act on simply supported beams laterally braced at the supports only. The lateral buckling length coefficient that represents the lateral bracing is equal to 1.0 (no lateral bracing for the beam). The results of the analysis are shown in Tables 3-6.

Classification of Section for Local Buckling

$\lambda_f = \dfrac{b}{t} = 9.58$ Width-to-Thickness ratio for a flange.

$\lambda_{fp} = 0.38 \sqrt{\dfrac{E}{Fy}} = 9.24$ Limiting slenderness for compact flange.

$\lambda_f > \lambda_{fp}$ the flange is non-compact.

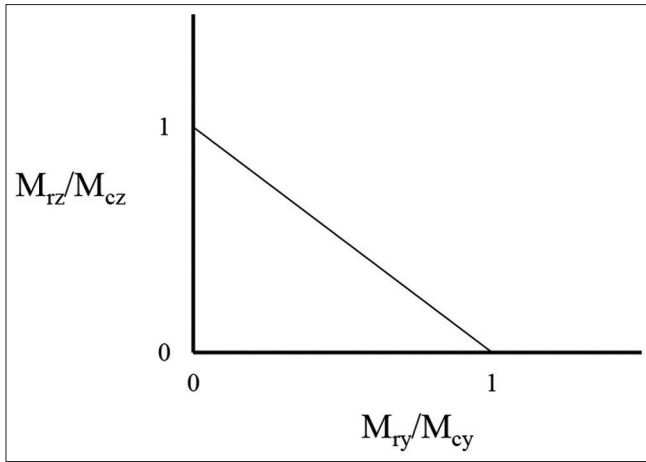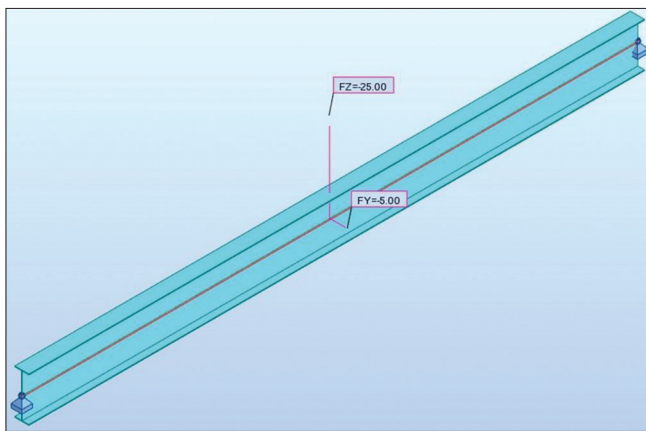**Figure 3:** Simple linear interaction for biaxial bending[2]

Figure 4: The case of the study

Table 1: Cross-section properties

Cross-section properties			
Symbul	**Values**	**Unit**	**Symbol description**
A_x	139.2	cm^2	Cross-section area
A_y	55.2	cm^2	Shear area – Y-axis
A_z	86.88	cm^2	Shear area – Z-axis
I_y	104264.9	cm^4	Second moment of area about the Y-axis
I_z	2443.48	cm^4	Second moment of area about the Z-axis
Z_y	3435.12	cm^3	Plastic section modulus about the Y (major) axis
S_y	2880.246	cm^3	Elastic section modulus about the Y-axis
Z_z	342.6	cm^3	Plastic section modulus about the Z (minor) axis
S_z	212.477	cm^3	Elastic section modulus about the Z-axis
d	72.4	cm	Cross-section height
b_f	23	cm	Cross-section width
t_f	1.2	cm	Thickness of Flange
t_w	1.2	cm	Web thickness

Table 2: Internal forces

Internal Forces	AISC	
	Vertical load	**Lateral load**
Applied factored Loads	40 kN	8 kN
Applied moment	y-axis	z-axis
	116 kN.m	20 N.m

$\lambda_w = \dfrac{h}{t_w} = 58.3$ Width-to-Thickness ratio for a web.

$\lambda_{wp} = 3.76\sqrt{\dfrac{E}{Fy}} = 91.45$ Limiting slenderness for compact web.

$\lambda_w < \lambda_{wp}$ ∴ the web is compact.

Parameters of Lateral Buckling Analysis

C_b = 1.32 lateral-torsional buckling modification factor, L_b =10 m laterally unbraced length of a member (lateral-torsional buckling), c = 1 for doubly symmetric section.

$r_{ts} = \sqrt{\dfrac{\sqrt{I_z C_w}}{S_y}} = 5.49$ cm, $h_0 = d - 2t_f = 70$ cm

$L_p = 1.76 r_z \sqrt{\dfrac{E}{F_y}} = 1.79$ Limiting laterally unbraced length for the

limit state of yielding.

$L_r = \dfrac{1.95 r_{ts} E}{0.7 F_y} \sqrt{\dfrac{Jc}{S_y h_0} + \sqrt{\left(\dfrac{Jc}{S_y h_0}\right)^2 + 6.76\left(\dfrac{0.7 F_y}{E}\right)^2}} = 5.3$ m Limiting

laterally unbraced length for the limit state of inelastic lateral-torsional buckling.

∵ $L_b > L_r$

∴ $F_{cr(LTB)} = \dfrac{C_b \pi^2 E}{\left(\dfrac{L_b}{r_{ts}}\right)^2}\sqrt{1 + 0.078\dfrac{Jc}{S_y h_0}\left(\dfrac{L_b}{r_{ts}}\right)^2} = 112.13$ MPa   (7)

F_{cr}: Critical stress (lateral-torsional buckling), J: torsional constant, c: Coefficient, S_y: Elastic section model.

$M_{ny(LTB)} = F_{cr(LTB)} \times S_y = 322.95$ KN.m Nominal lateral-torsional

buckling strength.

Eurocode Method of Analysis

In this method of analysis, the level where the load is applied must be defined, set the level of the applied load at Z = 1 in the member definition section beside the shape of bending moment in the load type section, the results of the analysis are shown in Tables 7-9.

Class of section

Flange: $c/t_f = 8.68 > 10\sqrt{\dfrac{235}{f_y}} = 8.1$ ∴ the flange is classified to

the third class.

Table 3: Cross-section properties required for AISC approach

Symbol	Values	Unit	Symbol description
A_x	139.2	cm^2	Cross-section area
A_y	55.2	cm^2	Shear area - Y-axis
A_z	86.88	cm^2	Shear area - Z-axis
J	66.82	cm^4	Torsional constant
Cw	3096768.81	cm^6	Warping constant
I_y	104264.9	cm^4	Moment of inertia of a section about the Y-axis
I_z	2443.48	cm^4	Moment of inertia of a section about the Z-axis
Z_y	3435.12	cm^3	Plastic section modulus about the Y (major) axis
S_y	2880.246	cm^3	Elastic section modulus about the Y-axis
Z_z	342.6	cm^3	Plastic section modulus about the Z (minor) axis
S_z	212.477	cm^3	Elastic section modulus about the Z-axis
d	72.4	cm	Height of cross-section
b_f	23	cm	Width of cross-section
t_f	1.2	cm	Flange thickness
t_w	1.2	cm	Web thickness
r_y	27.37	cm	Radius of gyration - Y-axis
r_z	4.19	cm	Radius of gyration - Z-axis

Table 4: Internal forces (AISC approach)

	Internal forces			
Symbul	Values	Unit	Symbol description	Section
M_{rz}	−20	kN.m	Required flexural strength	
V_{ry}	−4	kN	Required shear strength	
V_{rz}	−20	kN	Required shear strength	

Web: $c_w/t_w = 57.53 < 72\sqrt{\dfrac{235}{f_y}} = 58.58$ ∴ the web is

classified to the first class.

Lateral-torsional Buckling Analysis (General Method [6.3.2.2])

$L_{cr,upp}$ = 10 m upper flange, lateral bracing, C1=1.26 / C2=0.55 / C3 =1.73 factors, I_w=3096768.8 cm^6 warping constant, z_g = 36.2 cm From the shear center to the point of applied load.

$$M_{cr} = C_1 \frac{\pi^2 E I_z}{(K_z L)^2} \left\{ \left[\left(\frac{k_z}{k_w}\right)^2 \frac{I_w}{I_z} + \frac{G I_T}{\pi^2 E I_z} + \frac{(k_z L)^2}{(C_2 z_g - C_3 z_j)^2} \right]^{0.5} - (C_2 z_g - C_3 z_j) \right\} = 223.05$$

kN.m Critical moment for lateral-torsional buckling.

$\overline{\lambda_{LT}} = \sqrt{\dfrac{W_y f_y}{M_{cr}}} = 2.14$ Non-dimension slenderness ratio for lateral-torsional buckling.

Lateral buckling curve is **d** from Table 11.

α_{LT}=0.76 Imperfection factor for lateral buckling curves

Coefficient for calculation of $X_{LT.}$

$\chi_{LT} = \dfrac{1}{\phi_{LT} + \left(\phi_{LT}^2 - \overline{\lambda_{LT}}^2\right)^2} = 0.16$ Reduction factor for lateral-torsional buckling.

$M_{b.Rd} = \dfrac{\chi_{LT} W_y f_y}{\gamma_{M1}} = 161.39$ kN.m buckling resistance moment.

RESULTS

The main differences between AISC and Eurocode analysis results are explained in this section. Concern to the nominal strength, based on the results of the analysis, significant differences between the two approaches are demonstrated in Table 10.

As shown in Table 10, the difference between the design moment strengths of the Y-axis is 129.26 kN.m, where the section capacity regarding the AISC approach is approximately 80% higher than the Eurocode approach. The main reason for this would be due to the level of applied load, as this condition is not recognized by the AISC standard. AISC specifications take into consideration the level of applied load through the cross-section shear center, while this level would be under or above or just through the shear center considered by the Eurocode approach, this effect is demonstrated in Figure 5. The level of application of the load has a considerable effect on the elastic critical moment M_{cr}. To show this effect more, several sections with deferent depth and width but the same thickness of flange and web as listed below were tested.

Section 1: Total depth of beam = 724 mm, width of beam = 230 mm.

Section 2: Total depth of beam = 574 mm, width of beam = 250 mm (similar I section).

Section 3: Total depth of beam = 474 mm, width of beam = 400 mm (similar H section)

For all sections assumed that the level of the applied load at the upper part of the beam just on the flange with actual member definition for both approaches, the outcomes for this condition are shown in Figure 6.

This figure indicates that Section 3 which is similar to H sections would be the critical situation. To show an explanation for this huge difference between the two approaches, for both approaches the level of applied load places at the shear center of the cross-section (center of the section), and the modification factor C_b sets to one. The results of the analysis are shown in Figure 7.

The results are getting closer so that the first reason behind this difference in the computation is recognized which the AISC approach does not consider the level of applied

Table 5: Nominal strengths (AISC approach)

Symbul	Amounts	Unit	Symbol description	Section
Nominal strengths				
Respect to the Y axis				
M_{py}	1219.47	kN.m	Nominal plastic bending moment	[F]
M_{ny}[YD]	1219.47	kN.m	Nominal flexural strength in the limit state of yielding	[F3.1]
M_{ny}[LTB]	322.95	kN.m	Nominal lateral-torsional buckling strength	[F3.1]
$M_{ny}1$[LTB]	244.66	kN.m	Nominal lateral-torsional buckling strength (C_b=1.0)	[F3.1]
M_{ny}[FLB]	1203.48	kN.m	Nominal strength for local buckling of a compression flange	[F3.2]
M_{ny}	322.95	kN.m	Nominal flexural strength	[F3]
V_{nz}	1850.54	kN	Nominal shear strength	[G2.1]
Respect to the Z axis				
M_{pz}	121.62	kN.m	Nominal plastic bending moment	[F]
M_{nz}[YD]	120.69	kN.m	Nominal flexural strength in the limit state of yielding	[F6]
M_{nz}[FLB]	118.53	kN.m	Nominal strength for local buckling of a compression flange	[F6.2]
M_{nz}	118.53	kN.m	Nominal flexural strength	[F6]
V_{ny}	1175.76	kN	Nominal shear strength	[G2.1]

Table 6: Design strengths (AISC approach)

Symbol	Amounts	Unit	Symbol description	Section
Design strengths				
Respect to the Y axis				
Fib*M_{py}	1097.52	kN.m	Design plastic bending moment	[F]
Fib*M_{ny}[YD]	1097.52	kN.m	Design flexural strength in the limit state of yielding	[F3.1]
Fib*M_{ny}[LTB]	290.65	kN.m	Design lateral-torsional buckling strength	[F3.1]
Fib*$M_{ny}1$[LTD]	220.19	kN.m	Design lateral-torsional buckling strength	[F3.1]
Fib*M_{ny}[FLB]	1083.13	kN.m	Design strength for local buckling of a compression flange	[F3.2]
Fib*M_{ny}	290.65	kN.m	Design flexural strength	[F3]
Fiv*V_{nz}	1665.49	kN	Design shear strength	[G2.1]
Respect to the Z axis				
Fib*M_{pz}	109.46	kN.m	Design plastic bending moment	[F]
Fib*M_{nz}[YD]	108.62	kN.m	Design flexural strength in the limit state of yielding	[F6]
Fib*M_{nz}[FLB]	106.68	kN.m	Design strength for local buckling of a compression flange	[F6.2]
Fib*M_{nz}	106.68	kN.m	Design flexural strength	[F6]
Fiv*V_{ny}	1058.18	kN	Design shear strength	[G2.1]
Verification formulas				
UF (H1_1b)	0.59		$M_{ry}/(Fib*M_{ny}) + M_{rz}/(Fib*M_{nz})$	Verified
UF (G2_1)	0		$V_{ry}/(Fiv*V_{ny})$	Verified
UF (G2_1)	0.01		$V_{rz}/(Fiv*V_{nz})$	Verified

load unless when the load applied just on the top flange and for the case $L_b > Lr$ then the square root of Engineers[7] may conservatively takes one which does not take one in the analysis of Robot structural analysis software. In addition, other factors cause. Such as the type of section (rolled or welded) and the depth to width ratio(h/b), which is very effective in the case of lateral torsional buckling Table 11. The imperfection factor α_{LT} which is given in Table 12 covers the effect of lateral-torsional buckling that results in the redaction factor X_{LT} for the design moment capacity as shown in Velikovic *et al.*[8]
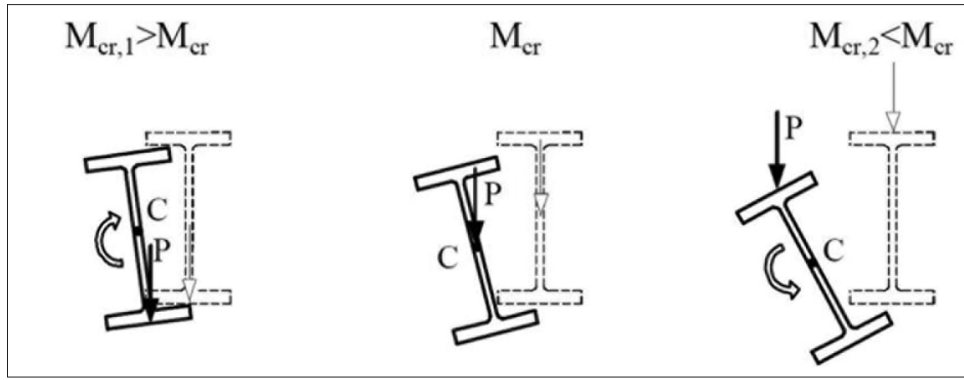
Figure 5: The influence of the level of the applied load on the capacity of the section
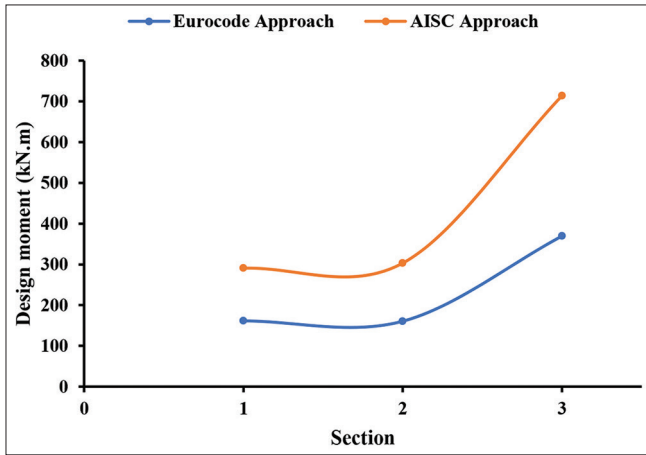

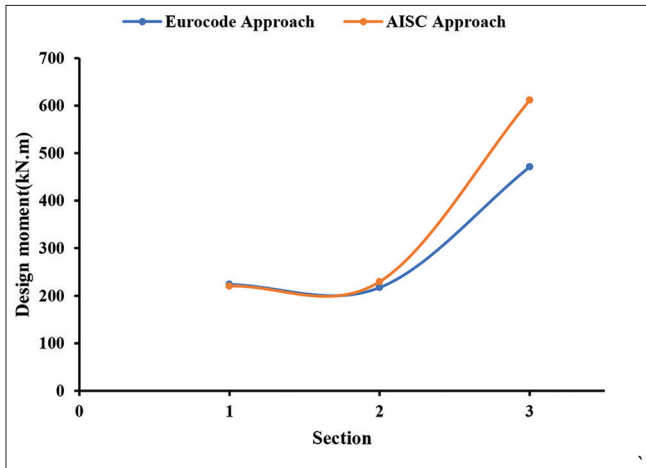**Figure 6:** Comparison of design moments about Y-axis with actual conditions

Figure 7: Comparison of design moments about y-axis with the load at the shear center for both approaches

$$\phi_{LT} = 0.5\left[1 + \alpha_{LT}\left(\overline{\lambda_{LT}} - 0.2\right) + \overline{\lambda_{LT}}^2\right] \tag{8}$$

$$\chi_{LT} = \frac{1}{\phi_{LT} + \left(\phi_{LT}^2 - \overline{\lambda_{LT}}^2\right)^2} \tag{9}$$

Table 7: Cross-section properties required for Eurocode approach

Symbol	Values	Unit	Section
A_x	139.2	cm²	
A_y	55.2	cm²	
A_z	84	cm²	
I_x	65.509	cm⁴	
I_y	104264.9	cm⁴	
I_z	2443.48	cm⁴	
W_{ely}	2880.246	cm³	
W_{elz}	212.477	cm³	
h	72.4	cm	
b	23	cm	
t_f	1.2	cm	
t_w	1.2	cm	
r_y	27.37	cm	
r_z	4.19	cm	
A_{nb}	1		(6.2.2.2)
E_{ta}	1		(6.2.6.(3))

Table 8: Internal forces

Internal forces				
Symbol	Values	Unit	Symbol description	Section
$M_{y, Ed}$	111.84	kN.m	Bending moment $M_{y.Ed}$	
$M_{z, Ed}$	−18.75	kN.m	Bending moment $M_{z.Ed}$	

$$M_{b.Rd} = \frac{\chi_{LT} W_y f_y}{\gamma_{M1}} \tag{10}$$

The rolled section performs better than the welded section. Table 2 shows that, because of the lateral load, the difference in the bending moment between two approaches around the Z-axis is about 31.25. Robot Structure Analysis software does not follow Fisher's concept, however, in most cases, Robot Structure Analysis software does not follow Fisher's concept, in most cases, the Eurocode approach is closer to the concept of Fisher. Fisher's concept is based on (2) and (3), where the nominal strength is

Table 9: Design forces and verifications

Symbol	Values	Unit	Symbol description	Section
Design forces				
$M_{b, Rd}$	161.39	kN.m	Buckling resistance moment	(6.3.2.1)
$M_{y, pl, Rd}$	1219.47	kN.m	Plastic resistance moment	(6.2.5.(2))
$M_{y, el, Rd}$	1022.49	kN.m	Elastic resistance moment	(6.2.5.(2))
$M_{y, c, Rd}$	1022.49	kN.m	Moment resistance	(6.2.5.(2))
$V_{y, c, Rd}$	1131.38	kN	Plastic shear resistance	(6.2.6.(2))
Respect to the Z axis z				
$M_{z, pl, Rd}$	121.62	kN.m	Plastic resistance moment	(6.2.5.(2))
$M_{z, el, Rd}$	75.43	kN.m	Elastic resistance moment	(6.2.5.(2))
$M_{z, c, Rd}$	75.43	kN.m	Moment resistance of a compressed section part	(6.2.5.(2))
$V_{z, c, Rd}$	1721.66	kN	Plastic shear resistance	(6.2.6.(2))
Verification formulas				
Global stability check of member				
UFB[M_yM_z] Ratio	0.94		$M_{y, Ed}/(X_{LT}*M_{y, Rk}/gM1) + M_{z, Ed}/(M_{z, Rk}/gM1)$	(6.3.3.(4))
RAT	0.94		Efficiency ratio	Section OK

Table 10: Comparison between AISC and Eurocode results

Approaches	AISC		Eurocode	
Design strength				
Notation	y- axis (kN.m)	z- axis (kN.m)	y- axis (kN.m)	z-axis (kN.m)
Design buckling resisting moment				
M_b, R_d	x	x	161.39	x
Design lateral-torsional buckling strength				
$F_{ib}*M_{ny}$	290.65	x	x	x
Moment resistance of a compressed section part				
$M_{z, c}, R_d$	x	x	x	75.43
Design strength for local buckling of a compression flange				
$F_{ib}*M_{nz}$	x	106.68	x	x

Table 11: Imperfection factor for lateral torsional buckling[8]

Buckling curve	a_o	a	b	c	d
Imperfection factor	0.13	0.21	0.34	0.49	0.76

Table 12: Buckling curves for lateral-torsional buckling (General method)

Section	Limits	Buckling curve
I or H sections rolled	$h/b \leq 2$	a
	$h/b \leq 2$	b
I or H sections welded	$h/b \leq 2$	c
	$h/b \leq 2$	d
Other sections	----	d

$$Z_t = \frac{Z_y}{2} = \frac{342.6}{2} = 171.3 \text{ cm}^3 \qquad (11)$$

$$M_{nt} = Z_t \times f_y = 171300 \times 355 = 60811500 \text{ N.mm} = 60.81 \text{kN.m} \qquad (12)$$
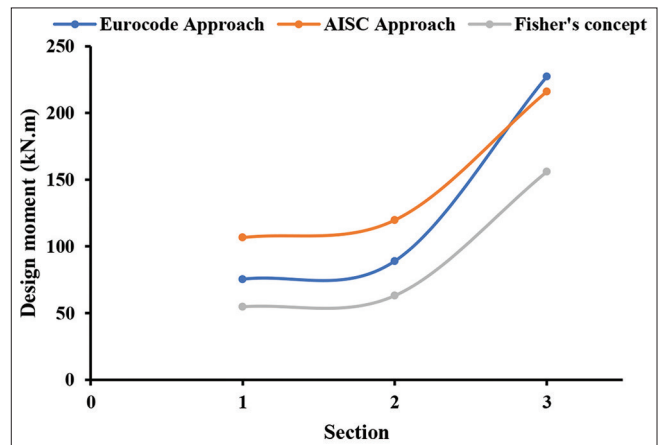

Figure 8: Comparison between the three approaches for design moment about Z-axis

The design moment capacity for section 1 is $\emptyset M_{nz} = 0.9(M_{nt}) = 0.9(60.81) = 54.72$ *kN.m*, and for sections
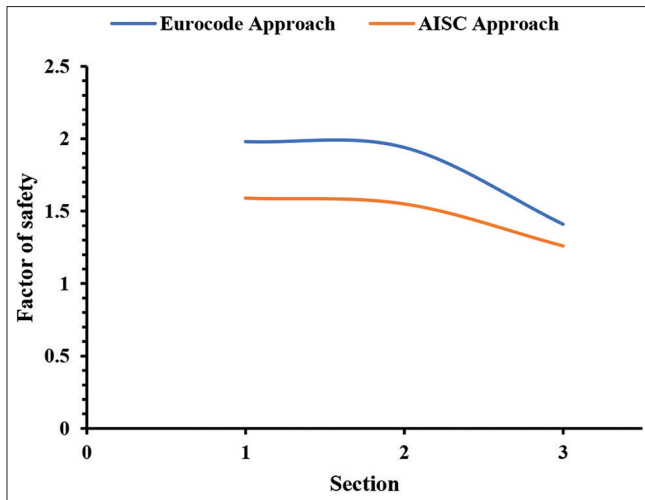
Figure 9: The difference in the factor of safety for biaxial bending manner

2 and 3 are 63.1 kN.m and 155.9 kN.m, respectively. The comparison between the three approaches is shown in Figure 8 Fisher's concept is more conservative than AISC and Eurocode methods of analysis. As shown, it is safer to use Fisher's concept or Eurocode approach in Robot structure Analysis software, Figuure 9 where the safety factor is defined as the ratio of the moment capacity of the section to the applied moment.

CONCLUSIONS

Based on the results of steel sections which analyzed by AISC and Eurocode standards, and Fisher's concept, the following points can be drawn:

1. Eurocode method of analysis results in more conservative design strength about Y-axis of the section as it takes into consideration the level where the loads are applied. On contrary, the AISC method of analysis does not take this effect into consideration unless when the load applied just on the top flange and for the case $L_b > Lr$ then the square root of equation (7) may conservatively takes one which does not take one in the analysis of Robot structural analysis software

2. Eurocode considers the lateral-torsional effect in terms of height/width ratio and the type of the section, rolled or welded, which results in the safety factor, which is not covered by AISC standards. The effect of lateral-torsional buckling and member type is much clear when the section is close to H-section

3. For the three types of sections (1, 2, and 3) considered in this study, Eurocode predicts design strength with safety factors of 1.98, 1.94, and 1.41, respectively, while such safety factors were 1.59, 1.54, and 1.26 for AISC approach. This concludes the adoption of Eurocode method of analysis in structural design of biaxial bending case when using Robot Structure Analysis software

4. Fisher's concept of structural design of biaxial bending of structural steel is more conservative than both AISC and Eurocode approaches of analysis.

REFERENCES

1. A. Ansi. AISC 360-16, Specification for Structural Steel Buildings, 2016.
2. A. Aghayere and J. Vigil. Structural Steel Design: Pearson India, 2008.
3. N. Boissonnade, R. Greiner, J. P. Jaspart and J. Lindner. Rules for Member Stability in EN 1993-1-1: Background Documentation and Design Guidelines, 2006.
4. L. Laim, J. P. C. Rodrigues and L. S. da Silva. Experimental and numerical analysis on the structural behaviour of cold-formed steel beams. *Thin Walled Structures*, vol. 72, pp. 1-13, 2013.
5. M. Fisher. Steel Design Guide 7: Industrial Buildings, Roofs to Anchor Rods. Chicago, IL: American Institute of Steel Construction, 2005.
6. Y. L. Pi and N. S. Trahair. Inelastic torsion of steel I-beams. *Journal of Structural Engineering*, vol. 121, pp. 609-620, 1995.
7. A. Engineers. Minimum Design Loads for Buildings and Other Structures, Standard Asce/Sei 7-10. Reston, VA: American Society of Civil Engineers, 2013.
8. M. Velikovic, L. S. da Silva, R. Simões, F. Wald, J. P. Jaspart, K. Weynand. Eurocodes: Background and Applications Design of Steel Buildings Worked Examples, Joint Research Center, 2015.